INSTITUTE OF PHYSICS PUBLISHING NONLINEARITY

Nonlinearity **18** (2005) 1655–1675 doi:10.1088/0951-7715/18/4/013

A variational principle based study of KPP minimal front speeds in random shears

James Nolen[1] **and Jack Xin**[2]

[1] Department of Mathematics, University of Texas, Austin, TX 78712, USA
[2] Department of Mathematics and ICES, Institute of Computational Engineering and Sciences, University of Texas, Austin, TX 78712, USA

E-mail: jnolen@math.utexas.edu and jxin@math.utexas.edu

Received 26 October 2004, in final form 4 April 2005
Published 29 April 2005
Online at stacks.iop.org/Non/18/1655

Recommended by K Ohkitani

Abstract

The variational principle for Kolmogorov–Petrovsky–Piskunov (KPP) minimal front speeds provides an efficient tool for statistical speed analysis, as well as a fast and accurate method for speed computation. A variational principle based analysis is carried out on the ensemble of KPP speeds through spatially stationary random shear flows inside infinite channel domains. In the regime of small root mean square (rms) shear amplitude, the enhancement of the ensemble averaged KPP front speeds is proved to obey the quadratic law under certain shear moment conditions. Similarly, in the large rms amplitude regime, the enhancement follows the linear law. In particular, both laws hold for the Ornstein–Uhlenbeck (O–U) process in the case of two-dimensional channels. An asymptotic ensemble averaged speed formula is derived in the small rms regime and is explicit in the case of the O–U process of the shear. The variational principle based computation agrees with these analytical findings, and allows further study of the speed enhancement distributions as well as the dependence of the enhancement on the shear covariance. Direct simulations in the small rms regime suggest a quadratic speed enhancement law for non-KPP nonlinearities.

Mathematics Subject Classification: 35K57, 41A60, 65D99

1. Introduction

Front propagation in heterogeneous fluid flows has been an active research topic for decades (see [7, 15, 18, 24–26, 28] and references therein). That the large time (large scale) front speed can be enhanced due to the presence of multiple scales in fluid flows is a fascinating phenomenon. Speed characterizations and enhancement laws have been studied mathematically for various flow patterns by analysis of the prototype models, e.g. the

reaction–diffusion–advection equations (see [3, 5, 8, 13, 16, 18–20, 22, 23, 25–27] and references therein). The enhancement obeys a quadratic law in the small amplitude flow regime, known as the Clavin–Williams relation [7], which was proved to be true for deterministic shear flows [13, 21–23]. The enhancement was proved to grow linearly in large amplitudes of deterministic flows (shear and percolating flows), see [4, 8, 11, 16, 21, 22]. However, an enhancement exponent of $\frac{4}{3}$ was reported based on numerical simulation of random Hamilton–Jacobi models (so called G-equation or KPZ models) on fronts in a weak randomly stirred array of vortices [16]. Likewise, the formal renormalization group method [28] suggested that front speeds may grow sublinearly (slower than linear by a logarithmic factor) in the strong random flow regime. These two findings raised the issue as to what extent the speed enhancement laws in the deterministic flows are valid for random flows. Recently, one of the present authors [27] showed that both the quadratic and linear laws hold almost surely for Kolmogorov–Petrovsky–Piskunov (KPP) minimal front speeds through white in time spatially Gaussian random shear flows on the plane. Yet the KPP front speeds diverge almost surely in spatially Gaussian random shears. A powerful tool is the variational principle of KPP minimal front speeds.

In this paper, we consider KPP front speeds through random shear flows in channel domains $D \equiv R \times \Omega$, where $\Omega \subset R^{n-1}$, $n \geqslant 2$, a bounded simply connected domain with a smooth boundary. We shall address the enhancement laws of the ensemble averaged front speeds. The model equation is:

$$u_t = \Delta_{x,y} u + B \cdot \nabla_{x,y} u + f(u), \tag{1.1}$$

where $t \in R^+$, $\Delta_{x,y}$ the n-dimensional Laplacian, $(x, y) \in D$. The nonlinearity $f = u(1-u)$, the so called KPP reaction. Other nonlinearities [26] will be discussed later. The vector field $B = (b(y, \omega), \mathbf{0})$, where $b(y, \omega)$, is a stationary continuous scalar random process in y, its ensemble mean equal to zero. The zero Neumann boundary condition is imposed at $\partial\Omega$: $\partial u/\partial \nu = 0$, ν is the unit outward normal.

For nonnegative initial data approaching zero and one at x infinities rapidly enough, the KPP solutions propagate as fronts with speed c^*, given by the variational principle [5, 6, 26],

$$c^* = c^*(\omega) = \inf_{\lambda > 0} \frac{\mu(\lambda, \omega)}{\lambda}, \tag{1.2}$$

where $\mu(\lambda, \omega)$ is the principal eigenvalue, with corresponding eigenfunction $\phi > 0$, of the problem:

$$\bar{L}_\lambda \phi = \Delta_y \phi + [\lambda^2 + \lambda b(y, \omega) + f'(0)]\phi = \mu(\lambda, \omega)\phi, \qquad y \in \Omega, \tag{1.3}$$

$$\frac{\partial \phi}{\partial \nu} = 0, \qquad y \in \partial\Omega. \tag{1.4}$$

The variational speed formula (1.2) makes possible an analysis of ensemble averaged random front speeds. Using variational formulae on the principal eigenvalue, μ, we are able to obtain tight upper and lower bounds on c^* and estimate $E[c^*]$ in terms of moments of suitable norms of the shear over Ω. For small root mean square (rms) shear, the quadratic enhancement law is proved and is explicit in the case of the Ornstein–Uhlenbeck (O–U) process when $n = 2$. The linear growth law holds in the large rms regime under weaker moment conditions on the shear. In both regimes, the moment conditions are satisfied by the O–U process when $n = 2$.

The variational formula (1.2) also offers an efficient and accurate way of computing a large ensemble of random front speeds. Directly solving the original time dependent equation (1.1) to obtain steady propagating states can be both slow and less accurate. A large ensemble of random fronts and occasional excursions in b require a large enough truncated channel domain

to contain the front over large times. As a result, direct simulation is prohibitively expensive in the regime of large rms shears.

The variational formula (1.2) allows us to compute quickly and accurately the ensemble averaged speeds in both small and large shear rms regimes when $n = 2$. An interesting difference from the deterministic case is that the integral average of $b(y, \omega)$ in $y \in \Omega$, i.e. $\bar{b} = \bar{b}(\omega) = |\Omega|^{-1} \int_\Omega b(y, \omega)\, dy$, is a random constant not equal to zero. This quantity can be of either sign, and influence greatly the numerical approximation of $E[c^*]$ in the small rms regime, even though it does not contribute to the exact $E[c^*]$, since $E[\bar{b}] = 0$. To assess the speed enhancement accurately, we subtract this random constant from each $c^*(\omega)$ before evaluating the expectation numerically. This way, we are able to minimize the errors in approximating $E[c^*]$ in a finite ensemble. In our computation, b is a discrete O–U process.

In complete agreement with analysis, we find numerically that the ensemble averaged speeds obey a quadratic law in the small rms regime and a linear law in the large rms regime. Without the $\bar{b}$ subtraction technique, the computed average speed enhancement in the small rms regime can give inaccurate scaling exponents significantly below 2. The same technique and direct simulations for other nonlinearities (combustion, bistable) suggest quadratic speed enhancement in the small rms regime. The computed speed ensemble then permits us to study further the enhancement distribution and its dependence on the variation of shear covariance functions.

This paper is organized as follows. In section 2, we prove the enhancement laws of ensemble averaged speeds based on variational principles, and derive a closed form speed asymptotic formula in the case of O–U process. In section 3, we describe numerical methods for computing a speed ensemble with the variational formula (1.2) and speed statistics and then show numerical results. We also make comparisons with the prediction of the asymptotic formula and with direct simulations. In section 4, we conclude with a remark on future work.

2. Average speed asymptotics

Consider a scaling shear amplitude $b(y) \mapsto \delta b(y)$, and denote by $c^*(\delta)$ the minimal KPP speed corresponding to shear δb. Let $c_0 = c^*(0) = 2\sqrt{f'(0)}$ denote the minimal speed in the case of zero advection. If the shear $b = b(y)$ has zero integral average over Ω, $\langle b \rangle = (1/|\Omega|) \int_\Omega b(y)\, dy = 0$, the corresponding minimal speed, $c^*(\omega)$, is always enhanced by the shear. This is true also for time dependent shears (see [21, 22] and references therein). For each realization, $c^*(\delta, \omega) = c_0^* + O(\delta^2)$ as $\delta \ll 1$; $c^*(\delta, \omega) = c_0^* + O(\delta)$ as $\delta \gg 1$. For each realization, as $\delta \ll 1$, we have:

Proposition 2.1. *Let $\chi = \chi(y)$ solve the equation $\Delta_y \chi = -b$, $y \in \Omega$, with zero Neumann boundary condition, where $b \in C(\overline{\Omega})$, has zero mean over Ω. Then for δ sufficiently small, the minimal speed has the expansion*

$$c^*(\delta) = c_0 + \frac{c_0 \delta^2}{2|\Omega|} \int_\Omega |\nabla \chi|^2\, dy + O(\delta^3). \tag{2.5}$$

Up to $O(\delta^2)$, the formula (2.5) is independent of the nonlinearity, see [13, 23] for f being bistable or combustion nonlinearity and [22] for more general nonlinearities and time periodic shears. We shall give a proof of proposition 2.1 using variational formulae, and later generalize it to the random case. That the infimum in (1.2) can be restricted to a bounded set independent of b and δ, as stated in the following lemma, is a helpful fact:

Lemma 2.1. *Let $b \in C(\overline{\Omega})$ have zero mean over Ω, and let $\lambda_0 = \sqrt{f'(0)}$. Then*

$$\inf_{\lambda > 0} \frac{\mu(\lambda)}{\lambda} = \inf_{0 < \lambda \leqslant \lambda_0} \frac{\mu(\lambda)}{\lambda}. \tag{2.6}$$

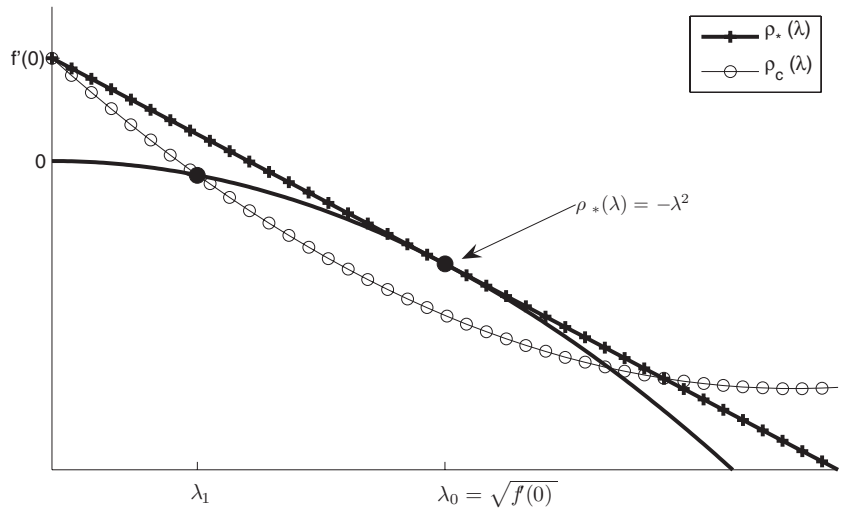

Figure 1. Intersecting curves ρ_c and $-\lambda^2$.

Proof. For each $c > 0$, we let $\rho_c(\lambda) = \mu(\lambda) - \lambda c - \lambda^2$. So, if $\phi > 0$ is the eigenfunction defined by (1.3), then $\rho_c(\lambda)$ is the principal eigenvalue defined by the equation

$$\Delta_y \phi + [\lambda b(y) - \lambda c + f'(0)]\phi = \rho_c(\lambda)\phi, \qquad y \in \Omega. \tag{2.7}$$

One can readily verify that $\partial_\lambda \rho_c(\lambda)|_{\lambda=0} = -c < 0$. The variational formula (1.2) can be expressed as

$$\begin{aligned} c^* &= \inf\{c|\exists \lambda > 0, \lambda c = \mu(\lambda)\} \\ &= \inf\left\{c|\exists \lambda > 0, \rho_c(\lambda) = -\lambda^2\right\}. \end{aligned} \tag{2.8}$$

Consider the points where $\rho_c(\lambda) = -\lambda^2$. By proposition 2.1 of [6], the continuous curve $\lambda \mapsto \rho_c(\lambda)$ is convex in λ, for each $c > 0$. Also, $\rho_c(0) = f'(0) > 0$. Therefore, for a given $c > 0$, there can be at most two values of $\lambda > 0$ such that $\rho_c(\lambda) = -\lambda^2$. The line $\rho_*(\lambda) = -2\sqrt{f'(0)}\lambda + f'(0)$ satisfies $\rho_*(\lambda) \geqslant -\lambda^2$, with equality holding only at one point: $\lambda_0 = \sqrt{f'(0)}$. Since $\rho_*(0) = \rho_c(0)$ and $\rho_c(\lambda)$ is convex and ρ_* is a line, $\rho_c(\lambda) = -\lambda^2$ for some $\lambda > 0$ only if $\rho_c(\lambda_1) = -\lambda_1^2$ for some $\lambda_1 \in (0, \lambda_0]$. This point is illustrated in figure 1. The solid curve represents the parabola $-\lambda^2$. If $\rho_c(\lambda)$ intersects $-\lambda^2$, then one of the intersection points must be to the left of $\lambda_0 = \sqrt{f'(0)}$. Therefore, from (2.8),

$$\left\{c|\exists \lambda > 0, \rho_c(\lambda) = -\lambda^2\right\} = \left\{c|\exists \lambda \in (0, \lambda_0], \rho_c(\lambda) = -\lambda^2\right\}. \tag{2.9}$$

So, we conclude that

$$c^*(\delta) = \inf_{0<\lambda} \frac{\mu(\lambda)}{\lambda} = \inf_{0<\lambda\leqslant\lambda_0} \frac{\mu(\lambda)}{\lambda}. \tag{2.10}$$

□

Proof of proposition 2.1. To estimate $c^*(\delta)$, we bound the principal eigenvalue $\mu(\lambda)$ using two different representations of μ. First, since $\bar{L}$ is a self-adjoint operator, we have

$$\mu = \sup \frac{(\bar{L}_\lambda \psi, \psi)}{\|\psi\|_2^2}, \tag{2.11}$$

where the supremum is taken over all $\psi \in H^2(\Omega)$ such that $\partial\psi/\partial\nu = 0$ on $\partial\Omega$. The other representation is

$$\mu = \inf_{\psi} \sup_{y\in\Omega} \frac{\bar{L}_\lambda \psi}{\psi} = \inf_{\psi} \sup_{y\in\Omega} \left(\frac{\Delta\psi}{\psi} + \lambda\delta b + \lambda^2 + f'(0) \right), \tag{2.12}$$

where the infimum can be taken over all $\psi \in C^1(\Omega)$ such that $\Delta\psi \in C(\Omega)$, $\psi > 0$ and $\partial\psi/\partial\nu = 0$ on $\partial\Omega$. This representation follows from the fact that the eigenfunction $\phi > 0$ lies in the kernel of the self-adjoint operator $(\bar{L}_\lambda - \mu(\lambda)I) = (\bar{L}_\lambda - \mu(\lambda)I)^*$. So, if we have the strict inequality

$$\bar{L}_\lambda \psi - \mu(\lambda)\psi = m < 0, \tag{2.13}$$

then the Fredholm alternative implies that $(\phi, m)_{L^2} = 0$, a contradiction since $\phi > 0, m < 0$. Hence,

$$\sup_{y\in\Omega} \frac{\bar{L}_\lambda \psi}{\psi} \geqslant \mu(\lambda). \tag{2.14}$$

Since $\bar{L}_\lambda \phi = \mu(\lambda)\phi$, the formula (2.12) follows. Note that we do not require the test functions ψ to be $C^2(\Omega)$, only $\Delta\psi \in C(\Omega)$. This is important since we do not want to require the shear $b(y)$ to be any more regular than $b \in C(\bar{\Omega})$.

Let us derive upper and lower bounds for $\mu(\lambda)$ by choosing test functions ψ as

$$\psi = 1 + \lambda\delta\chi + \lambda^2\delta^2 h, \tag{2.15}$$

where $\chi = \chi(y)$ and $h = h(y)$ solve

$$\begin{aligned} \Delta\chi &= -b, \\ \Delta h &= -b\chi + k, \end{aligned} \tag{2.16}$$

with zero Neumann boundary conditions at $\partial\Omega$, and k a constant equal to

$$k = \frac{1}{|\Omega|}\int_\Omega b\chi \,\mathrm{d}y = \frac{1}{|\Omega|}\int_\Omega |\nabla\chi|^2 \,\mathrm{d}y. \tag{2.17}$$

We normalize χ and h so that

$$\inf_{x\in\Omega} \chi(x) = 0 \qquad \text{and} \qquad \inf_{x\in\Omega} h(x) = 0. \tag{2.18}$$

Then

$$\bar{L}_\lambda \psi = \lambda^2\delta^2 k + \lambda^3\delta^3 bh + (\lambda^2 + f'(0))\psi$$

and

$$\frac{(\bar{L}_\lambda\psi, \psi)}{\|\psi\|_2^2} = \lambda^2\delta^2 k \frac{\int\psi}{\int\psi^2} + \lambda^3\delta^3 \frac{\int bh\psi}{\int\psi^2} + \lambda^2 + f'(0). \tag{2.19}$$

Using the definition of ψ, we see that $\psi = \psi^2 - \lambda\delta\chi\psi - \lambda^2\delta^2 h\psi$ and

$$\frac{\int_\Omega \psi \,\mathrm{d}y}{\int_\Omega \psi^2 \,\mathrm{d}y} = 1 - \lambda\delta \frac{\int_\Omega \chi\psi \,\mathrm{d}y}{\int_\Omega \psi^2 \,\mathrm{d}y} - \lambda^2\delta^2 \frac{\int_\Omega h\psi \,\mathrm{d}y}{\int_\Omega \psi^2 \,\mathrm{d}y}.$$

Now from (2.11) and (2.19) we have the lower bound

$$\mu(\lambda) \geqslant \lambda^2 + f'(0) + \lambda^2\delta^2 k + R_1 \tag{2.20}$$

with

$$R_1 = -\frac{\lambda^3\delta^3}{\int_\Omega \psi^2} \left(k\int_\Omega \chi\psi + k\lambda\delta \int_\Omega h\psi - \int_\Omega bh\psi \right). \tag{2.21}$$

By choice of $\chi \geqslant 0$ and $h \geqslant 0$, we have $\int_\Omega \psi^2 \geqslant |\Omega|$ for all $\delta \geqslant 0$ and $\lambda > 0$. Hence, $R_1 = O(\delta^3)$ for λ bounded. Returning to the variational formula (2.10), we now have a lower bound on $c^*(\delta)$:

$$\begin{aligned} c^*(\delta) = \inf_{0<\lambda\leqslant\lambda_0} \frac{\mu(\lambda)}{\lambda} &\geqslant \inf_{0<\lambda\leqslant\lambda_0} \left(\lambda + \frac{f'(0)}{\lambda} + \lambda\delta^2 k + \frac{R_1}{\lambda}\right) \\ &\geqslant \inf_{\lambda>0} \left(\lambda + \frac{f'(0)}{\lambda} + \lambda\delta^2 k\right) + O(\delta^3) \\ &= 2\sqrt{f'(0)(1+\delta^2 k)} + O(\delta^3) \\ &= c_0 + \frac{c_0\delta^2 k}{2} + O(\delta^3). \end{aligned} \tag{2.22}$$

To obtain an upper bound on $c^*(\delta)$, we use (2.12) and calculate

$$\begin{aligned} \frac{\bar{L}_\lambda \psi}{\psi} &= \frac{\Delta\psi}{\psi} + \lambda\delta b + \lambda^2 + f'(0) \\ &= \frac{\lambda^2\delta^2 k + \lambda^3\delta^3 bh}{1 + \lambda\delta\chi + \lambda^2\delta^2 h} + \lambda^2 + f'(0). \end{aligned} \tag{2.23}$$

Since $\chi \geqslant 0$ and $h \geqslant 0$, we see from (2.12) and (2.23) that

$$\mu(\lambda) \leqslant \sup_{y\in\Omega} \frac{\bar{L}_\lambda \psi}{\psi} \leqslant \lambda^2 + f'(0) + \lambda^2\delta^2 k + R_2 \tag{2.24}$$

with

$$R_2 = \lambda^3\delta^3 \|bh\|_\infty. \tag{2.25}$$

The variational formula (2.10) implies

$$\begin{aligned} c^*(\delta) = \inf_{0<\lambda\leqslant\lambda_0} \frac{\mu(\lambda)}{\lambda} &\leqslant \inf_{0<\lambda\leqslant\lambda_0} \left(\lambda + \frac{f'(0)}{\lambda} + \lambda\delta^2 k + R_2\right) \\ &= c_0 + \frac{c_0\delta^2 k}{2} + O(\delta^3), \end{aligned} \tag{2.26}$$

thus completing the proof. □

When the shear $b(y, \omega)$ is a random process, the corresponding minimal speed $c^*(\delta) = c^*(\delta, \omega)$ is a random variable for each δ, and we consider how the expectation $E[c^*(\delta)]$ scales with the parameter δ by finding an exponent p such that $E[c^*(\delta)] = c^*(0) + O(\delta^p)$. Each realization of the process $b(y, \omega)$ restricted to the domain Ω does not necessarily have zero integral over Ω. Nevertheless, each realization can be written in the form

$$b(y, \omega) = \bar{b}(\omega) + b_1(y, \omega), \tag{2.27}$$

where $\bar{b}(\omega) = \langle b(y, \omega)\rangle$ is the mean of b over Ω, and $b_1(y, \omega)$ is the variation about the mean value. For a fixed realization, the minimal speed $c^*(\delta)$ will be affected by both the scaling of the mean $\bar{b}(\omega)$ and the scaling of the variation $b_1(y, \omega)$. That is,

$$c^*(\delta, \omega) = c_0^* + \delta\bar{b}(\omega) + M(\delta, \omega), \tag{2.28}$$

where the remainder $M(\delta, \omega)$ is the enhancement due to the variation $b_1(y, \omega)$, different for each realization. Taking the expectation of both sides of (2.28), we have

$$E[c^*(\delta)] = c_0^* + \delta E[\bar{b}(\omega)] + E[M(\delta, \omega)]. \tag{2.29}$$

For each sample, $M(\delta, \omega)$ is $O(\delta^2)$ for δ small. Though $E[M(\delta)]$ might exhibit scaling different from quadratic, we show that the quadratic scaling law remains for enhancement of averaged front speeds under suitable moment conditions of the shear.

Theorem 2.1. *Let $b(y, \omega)$ be a stationary random process in R^{n-1} ($n \geqslant 2$) so that its sample paths are almost surely continuous and*

$$E[\|b\|_\infty^6] < +\infty. \tag{2.30}$$

Then for δ small, the expectation $E[c^*(\delta)]$ has the expansion

$$E[c^*(\delta)] = c_0 + \delta E[\langle b\rangle] + \frac{c_0\delta^2}{2|\Omega|}\int_\Omega E[|\nabla\chi|^2]\,\mathrm{d}y + O(\delta^3), \tag{2.31}$$

where $b(y, \omega) = \langle b\rangle(\omega) + b_1(y, \omega)$; and $\chi = \chi(y, \omega)$ solves $\Delta_y\chi = -b_1$, $y \in \Omega$, subject to zero Neumann boundary condition.

Proof. As the contribution of $\langle b\rangle$ to c^* is just an additive constant, it suffices to consider shear flow b_1 and show that it gives the averaged speed

$$E[c^*(\delta)] = c_0 + \frac{c_0\delta^2}{2|\Omega|}\int_\Omega E[|\nabla\chi|^2]\,\mathrm{d}y + O(\delta^3). \tag{2.32}$$

We adapt the proof of proposition 2.1, noting that in the stochastic case the remainders R_1 and R_2 defined by (2.21) and (2.25) are random and not bounded uniformly for all realizations. Instead, we will show that for λ in a bounded interval,

$$E[|R_1|] \leqslant O(\delta^3) \qquad \text{and} \qquad E[|R_2|] \leqslant O(\delta^3).$$

To this end, we estimate χ and h, with C denoting a generic positive constant depending only on the domain Ω and its dimension. Let χ and h solve (2.16) with $\langle\chi\rangle = \langle h\rangle = 0$. Applying $W^{2,p}$ estimates [9, 10], we have

$$\|\chi\|_{W^{2,p}(\Omega)} \leqslant C\|b_1\|_{L^p(\Omega)} \leqslant C|\Omega|^{1/p}\|b_1\|_\infty \tag{2.33}$$

and

$$\begin{aligned}\|h\|_{W^{2,p}(\Omega)} &\leqslant C\|b_1\chi + k\|_{L^p(\Omega)}\\ &\leqslant C\|b_1\|_\infty\|\chi\|_{L^p(\Omega)} + Ck|\Omega|^{1/p}\\ &\leqslant C\|b_1\|_\infty^2\end{aligned} \tag{2.34}$$

since

$$k = \langle|\nabla\chi|^2\rangle \leqslant C\|b_1\|_\infty^2. \tag{2.35}$$

Given $\alpha \in (0, 1)$, we can choose $p > 1$ sufficiently large, depending on n, such that $W^{2,p}(\Omega)$ embeds continuously into $C^{1,\alpha}(\bar\Omega)$. It follows that there is a constant $C > 0$ independent of b such that

$$\|\chi\|_{C^1(\bar\Omega)} \leqslant C\|b_1\|_\infty \qquad \text{and} \qquad \|h\|_{C^1(\bar\Omega)} \leqslant C\|b_1\|_\infty^2. \tag{2.36}$$

If instead we normalize χ and h by (2.18), then the bounds (2.36) still hold, with different constants. Note that adding a constant to χ and h does not alter the quantity $\int_\Omega|\nabla\chi|^2$ that appears in the asymptotic expansion.

Now by (2.36), the integrals in R_1 are easily bounded as

$$\begin{aligned}\int_\Omega\chi\psi &= \int_\Omega\chi + \lambda\delta\chi^2 + \lambda^2\delta^2\chi h\\ &\leqslant C\left(\|b_1\|_\infty + \lambda\delta\|b_1\|_\infty^2 + \lambda^2\delta^2\|b_1\|_\infty^3\right).\end{aligned}$$

Similarly,

$$\begin{aligned}\int_\Omega h\psi &= \int_\Omega h + \lambda\delta\chi h + \lambda^2\delta^2h^2\\ &\leqslant C\left(\|b_1\|_\infty^2 + \lambda\delta\|b_1\|_\infty^3 + \lambda^2\delta^2\|b_1\|_\infty^4\right)\end{aligned}$$

and

$$\left|\int_\Omega b_1 h\psi \,\mathrm{d}y\right| = \left|\int b_1 h + \lambda\delta \int b_1 h\chi + \lambda^2\delta^2 \int b_1 h^2\right| \leqslant C\left(\|b_1\|_\infty^3 + \lambda\delta\|b_1\|_\infty^4 + \lambda^2\delta^2\|b_1\|_\infty^5\right).$$

Since χ and h are nonnegative, $\int_\Omega \psi^2 \mathrm{d}y \geqslant C\int_\Omega \psi = C|\Omega| > 0$ for any realization. So for λ in a bounded interval and δ small, we bound (2.21) by

$$|R_1| \leqslant C\delta^3\lambda^3(1 + \|b_1\|_\infty^6),$$

so that $E[|R_1|] \leqslant O(\delta^3)$.

To bound $E[|R_2|]$, we use the normalization (2.18) and the above estimates:

$$|R_2| = \lambda^3\delta^3 \|b_1 h\|_\infty \leqslant C\,\lambda^3\delta^3\,\|b_1\|_\infty^3. \tag{2.37}$$

Hence $E[R_2] \leqslant O(\delta^3)$ for λ in a finite interval. Now we return to (2.22) to conclude

$$E[c^*(\delta)] \geqslant E\left[2\sqrt{f'(0)(1+\delta^2 k)}\right] + O(\delta^3) = c_0 + \frac{c_0\delta^2 E[k]}{2} + O(\delta^3)$$

since $E[k^2] \leqslant C\,E[\|b\|_\infty^4] < \infty$.

The opposite inequality follows from (2.26) since $E[R_2] = O(\delta^3)$ for $\lambda \in (0, \lambda_0)$. Thus formula (2.32) holds. For general b, not necessarily mean zero,

$$E[c^*(\delta)] = c_0 + \delta E[\langle b\rangle] + \frac{c_0\delta^2}{2}E[k] + O(\delta^3) = c_0 + \delta E[\langle b\rangle] + \frac{c_0\delta^2}{2|\Omega|}\int_\Omega E[|\nabla\chi|^2]\,\mathrm{d}y + O(\delta^3).$$

The proof is complete. □

In our numerical computation of front speeds in two-dimensional channels, we use the O–U process for shear b, and so $E[\langle b\rangle] = 0$. Let us show below that the O–U process, denoted by $X(y, \omega)$, satisfies the conditions in theorem 2.1, and so $E[c^*(\delta)]$ scales quadratically with δ for δ small.

Corollary 2.1 (explicit average speed formula). *Consider the O–U process $b(y, \omega)$ as a solution of the Ito equation:*

$$\mathrm{d}X(y) = -aX(y)\,\mathrm{d}y + r\,\mathrm{d}W(y), \qquad y \in [0, L], \tag{2.38}$$

where $W(y, \omega)$ is the standard Wiener process, $X(0, \omega) = X_0(\omega)$ is a Gaussian random variable with mean zero and variance $\rho = r^2/(2a)$. Then $X(y, \omega)$ satisfies the moment conditions in theorem 2.1. The averaged KPP front speed in the channel $R \times [0, L]$ is given by

$$E[c^*(\delta)] = c_0 + \frac{c_0\delta^2}{2}\,\mathrm{enh} + O(\delta^3), \qquad \delta \ll 1, \tag{2.39}$$

where

$$\mathrm{enh} = \frac{r^2}{2a}\left(\mathrm{e}^{-aL}\left(\frac{4}{L^2a^4} - \frac{1}{3a^2}\right) + \frac{L}{3a} - \frac{4}{L^2a^4} - \frac{5}{3a^2} + \frac{4}{La^3}\right).$$

Proof. The O–U process is stationary and Markov. Its sample paths are almost surely Hölder continuous though nowhere differentiable. The process can be written as

$$b(y, \omega) = \mathrm{e}^{-ay}b(0, \omega) + r\int_0^y \mathrm{e}^{-a(y-s)}\,\mathrm{d}W_s(\omega). \tag{2.40}$$

The covariance function of this process is $\rho e^{-a|y-s|}$. Letting $g(y,\omega)$ denote the process

$$g(y) = e^{ay} b(y,\omega) = g(0,\omega) + r\int_0^y e^{as}\,dW_s(\omega), \tag{2.41}$$

we see that $g(y,\omega)$ is a martingale [14]. By Doob's martingale moment inequality [14], for any $p \in (1,+\infty)$,

$$E[\sup_{0<y<L}|g(y)|^p] \leqslant \left(\frac{p}{p-1}\right)^p E[|g(L)|^p]. \tag{2.42}$$

Since the process $b(y,\omega)$ is Gaussian, (2.41) and (2.42) imply that

$$E[\|b\|_\infty^6] \leqslant C\,E[|b(L)|^6] < +\infty. \tag{2.43}$$

Formula (2.39) now applies to the average speed. Note that

$$(\chi_x(x))^2 = \int_0^x\int_0^x b_1(s)b_1(y)\,ds\,dy$$

and

$$E[(\chi_x(x))^2] = \int_0^x\int_0^x E[b_1(s)b_1(y)]\,ds\,dy. \tag{2.44}$$

Let us calculate $E[b_1(s)b_1(y)]$ in terms of $E[b(s)b(y)]$. Define

$$g(y) = \langle f(\cdot,y)\rangle \qquad \text{or} \qquad g(s) = \langle f(s,\cdot)\rangle,$$

so that

$$E[b_1(y)b_1(s)] = E[b(s)b(y)] - E[b(s)\bar{b}] - E[b(y)\bar{b}] + E[\bar{b}^2],$$

$$E[b(s)\bar{b}] = \frac{1}{L}\int_0^L E[b(y)b(s)]\,dy = g(s),$$

$$E[\bar{b}^2] = \frac{1}{L^2}\int_0^L\int_0^L E[b(s)b(y)]\,dy\,ds = \langle g\rangle.$$

Thus

$$E[b_1(y)b_1(s)] = f(s,y) + \langle g\rangle - g(y) - g(s).$$

Now, we have

$$\begin{aligned} E[(\chi_x(x))^2] &= \int_0^x\int_0^x E[b_1(s)b_1(y)]\,ds\,dy \\ &= \int_0^x\int_0^x f(s,y) + \langle g\rangle - g(y) - g(s)\,ds\,dy \\ &= x^2\langle g\rangle - 2x^2\langle g\rangle_x + \int_0^x\int_0^x f(s,y)\,ds\,dy, \end{aligned}$$

where $\langle g\rangle_x$ denotes the average of g over the interval $[0,x]$, for $0 < x \leqslant L$. Consequently, we have

$$E[\langle|\chi_x|^2\rangle] = \frac{1}{L}\int_0^L \left(x^2\langle g\rangle - 2x^2\langle g\rangle_x + \int_0^x\int_0^x f(s,y)\,ds\,dy\right)dx. \tag{2.45}$$

Using the O–U covariance function, we proceed as

$$\begin{aligned} g(s) &= \frac{1}{L}\int_0^L f(s,y)\,dy = \frac{r^2}{2a}\frac{1}{L}\int_0^L e^{-a|y-s|}\,dy \\ &= \frac{r^2}{2a}\left(\frac{1-e^{-as}}{La} + \frac{1-e^{-a(L-s)}}{La}\right) \end{aligned}$$

and

$$\langle g\rangle_x = \frac{r^2}{2a}\frac{1}{x}\int_0^x \left(\frac{1-\mathrm{e}^{-as}}{La} + \frac{1-\mathrm{e}^{-a(L-s)}}{La}\right)\mathrm{d}s$$
$$= \frac{r^2}{2a}\left(\frac{2}{La} + \frac{1}{xLa^2}(\mathrm{e}^{-ax}-1) + \frac{1}{xLa^2}(\mathrm{e}^{-aL}-\mathrm{e}^{-a(L-x)})\right).$$

Letting $x = L$, we have

$$\langle g\rangle = \frac{r^2}{2a}\left(\frac{2}{La} + \frac{2}{L^2a^2}(\mathrm{e}^{-aL}-1)\right).$$

Similarly,

$$\int_0^x\int_0^x f(s,y)\,\mathrm{d}s\,\mathrm{d}y = \frac{r^2}{2a}\left(\frac{2x}{a} + \frac{2}{a^2}(\mathrm{e}^{-ax}-1)\right).$$

Combining the above, we have

$$E[\langle|\chi_x|^2\rangle] = \frac{r^2}{2a}\left(\frac{2L}{3a} + \frac{2}{3a^2}(\mathrm{e}^{-aL}-1)\right)$$
$$-\frac{r^2}{2a}\frac{2}{L}\int_0^L \frac{2x^2}{La} + \frac{x}{La^2}(\mathrm{e}^{-ax}-1) + \frac{x}{La^2}(\mathrm{e}^{-aL}-\mathrm{e}^{-a(L-x)})\,\mathrm{d}x$$
$$+\frac{r^2}{2a}\frac{1}{L}\int_0^L \frac{2x}{a} + \frac{2}{a^2}(\mathrm{e}^{-ax}-1)\,\mathrm{d}x$$
$$= \frac{r^2}{2a}\left(\mathrm{e}^{-aL}\left(\frac{4}{L^2a^4} - \frac{1}{3a^2}\right) + \frac{L}{3a} - \frac{4}{L^2a^4} - \frac{5}{3a^2} + \frac{4}{La^3}\right). \tag{2.46}$$

In view of (2.39), the proof is complete. □

Theorem 2.2 (linear growth). *If the stationary shear process $b(y,\omega)$ has almost surely continuous sample paths and satisfies $E[\|b\|_\infty] < \infty$, then the amplified shear field $\delta b(y,\omega)$ generates the average front speed:*

$$E[|c^*(\delta,\omega)|] = O(\delta), \qquad \delta \gg 1.$$

Moreover, $\lim_{\delta\to\infty} E[|c^*(\delta,\omega)|]/\delta$ *exists.*

Proof. By theorem 5.1 of [4], $|c^*(\delta,\omega)|/\delta \to d^*(\omega)$ as $\delta\to\infty$, where d^* is finite for each ω. Now recall the upper bound $|c^*(\delta,\omega)| \leqslant |c_0| + \delta\|b\|_\infty$. Hence for $\delta > |c_0|$, $|c^*(\delta,\omega)|\delta \leqslant 1+\|b\|_\infty \equiv Y$ and $E(Y) < \infty$. The dominated convergence theorem implies that

$$E\left[\frac{|c^*(\delta,\omega)|}{\delta}\right] \to E[d^*(\omega)] \leqslant E(Y).$$

The proof is complete. Clearly, the O–U process satisfies the required condition for linear average speed growth. □

Remark 2.1. The limiting value or the linear growth rate, $d^*(\omega)$, depends on $b(y,\omega)$ in a rather implicit way. After completion of this work, the authors learned of a recent variational formula by Heinze [12]:

$$d^*(\omega) = \sup_{\psi\in D_1}\int_\Omega b(y,\omega)\psi^2(y)\,\mathrm{d}y,$$

where

$$D_1 = \{\psi\in H^1(\Omega)\colon \|\nabla\psi\|_2^2 \leqslant f'(0),\ \|\psi\|_2 = 1\}.$$

If a realization of b were to have a flat piece near the maximal point of b in Ω, $d^*(\omega)$ would be equal to $\sup_\Omega b(y,\omega)$. However, this happens with zero probability for the O–U process among other stationary Gaussian random fields. It appears that the distribution of $d^*(\omega)$ is analytically unknown. In fact, even the distribution of $\sup_\Omega b(y,\omega)$ is known only in a few special cases [1], not including O–U. For this reason, an efficient numerical technique like the one described in the following section is very useful for analysis of the statistical behaviour of $c^*(\delta)$ as $\delta \to \infty$.

3. Computation by variational principle

3.1. Numerical methods

Let $n = 2$. For a given $\lambda > 0$, we compute the principal eigenvalue, $\mu(\lambda)$, with corresponding eigenfunction $\phi = \phi(y) > 0$, $y \in [0, L]$, by solving

$$\begin{aligned} &\phi_{yy} + [\lambda^2 + \lambda b(y) + f'(0)]\phi = \mu(\lambda)\phi, \qquad y \in (0, L), \\ &\frac{\partial \phi}{\partial y} = 0, \qquad y = 0, L, \end{aligned} \tag{3.1}$$

using a standard second-order finite-difference method. Here we suppress the random parameter ω, as computation is done realization by realization. Denote the uniform partition of the domain by points $\{y_i\}_{i=1}^m$, and the numerical solution by $\bar\phi = \{\bar\phi_i\}_{i=1}^m$, where $h = L/(m-1)$, $y_i = (i-1)h$ and $\bar\phi_i \approx \phi(y_i)$. The discretized system is

$$\frac{1}{h^2}\bar\phi_{i-1} + \left(\lambda^2 + \lambda b_i + f'(0) - \frac{2}{h^2}\right)\bar\phi_i + \frac{1}{h^2}\bar\phi_{i+1} = \mu(\lambda)\bar\phi_i \qquad i = 2, \ldots, m-1,$$

with second-order approximation of the Neumann boundary conditions. This reduces to finding the principal eigenvalue of a symmetric tridiagonal matrix, easily accomplished with double precision LAPACK routines [2]. Then we compute points on the curve $H(\lambda) = \mu(\lambda)/\lambda$ and minimize over λ using Newton's method with line search. Our approximation decreases with each iteration and converges quadratically in the region near the infimum. Two illustrative curves, $H(\lambda)$, are shown in figure 2 for two different realizations of the shear.

We generate realizations of the shear process $b(y,\omega)$ by numerically evaluating the stochastic ODE (2.38) with the Milstein scheme (see [17]). Although this scheme is first order, we use a discrete spacing $\bar h \leqslant h^2$, where h is the discrete grid spacing for the eigenvalue problem, so that the method is still second order accurate in the parameter h. Figure 3 shows a sample path, and figure 4 compares exact and numerical covariance functions constructed from 5000 samples.

To approximate the expectation $E[c^*(\delta)]$, we generate N independent realizations (indexed by $i = 1, \ldots, N$) of the shear and compute the corresponding minimal speeds $\{c_i^*\}$ for each δ. Then we compute the average,

$$E[c^*(\delta)] \approx \bar E(\delta) = c_0^* + \frac{1}{N}\sum_{i=1}^{N} M_i(\delta), \tag{3.2}$$

where $M_i(\delta) = c_i^*(\delta) - c_0^* - \delta\bar b_i$. That is, we subtract the linear part due to the mean of the shear being nonzero, as in (2.28).

Once we have the averages $\bar E(\delta)$ for each δ, we compute the exponents p using the least squares method to fit a line to a log–log plot of speed versus amplitude. That is, the exponent p is the slope of the best-fit line through the data points $(\log(\delta), \log(\bar E[c^*(\delta)] - c^*(0)))$ for each shear amplitude δ.

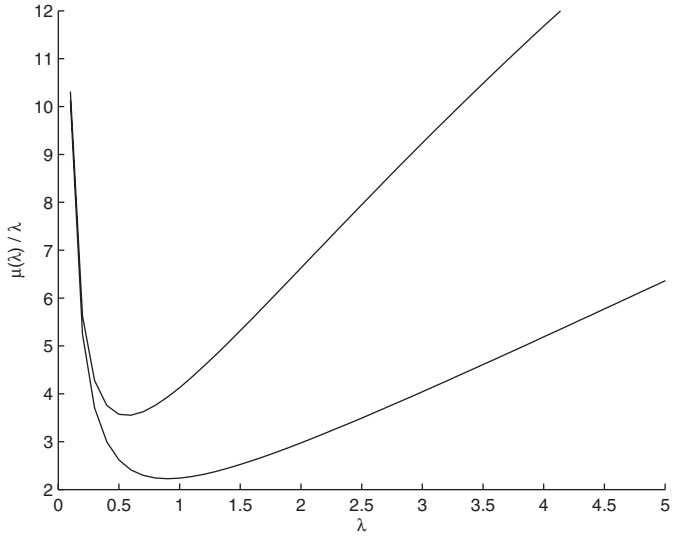

Figure 2. Two curves $\lambda \mapsto \mu(\lambda)/\lambda$.

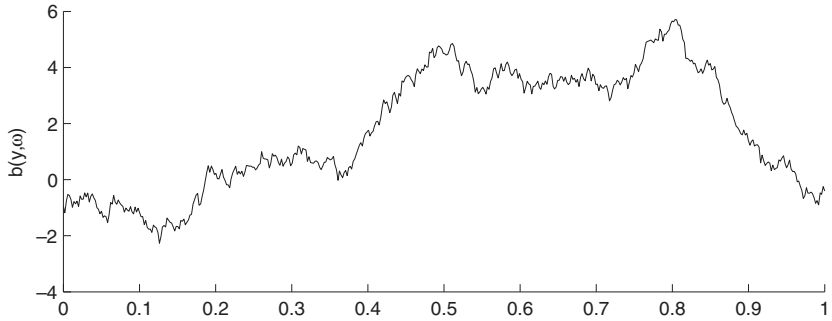

Figure 3. One sample path of the O–U process $b(y, \omega)$.

3.2. Numerical results

3.2.1. Scaling with shear amplitude δ. In figures 5 and 6, we show the results of a simulation using $N = 100\,000$ realizations of a shear in small and large rms amplitudes, respectively. As shown later in figure 11, we find that the choice of $N = 100\,000$ samples was more than enough to obtain good convergence of the speed distribution functions. The covariance function of the process is $E[b(y)b(s)] = 2e^{-4|y-s|}$. In each plot, we show multiple curves, corresponding to various domain sizes. In figure 5, corresponding to small δ, the solid curves are the numerically computed values; the dotted curves are given by formula (2.39). We find that the enhancement of the minimal speed scales quadratically for small amplitudes and linearly for large amplitudes. The computed exponents are shown in table 1.

As an application of the numerical results for large amplitudes, we compare the distribution of $c^*(\delta)$ with the distributions of the random variables $g_1(\omega) = 2\kappa f'(0) + \delta\|b\|_\infty$ and $g_2(\omega) = 2\sqrt{\kappa + \delta^2/\kappa\|\nabla\chi\|_\infty}$, where κ is the diffusion constant (equal to 1 in equation (1.1)). Theorem 2 of [11] shows the upper bound:

$$c^*(\delta, \omega) \leqslant \min(g_1(\omega), g_2(\omega)) \tag{3.3}$$

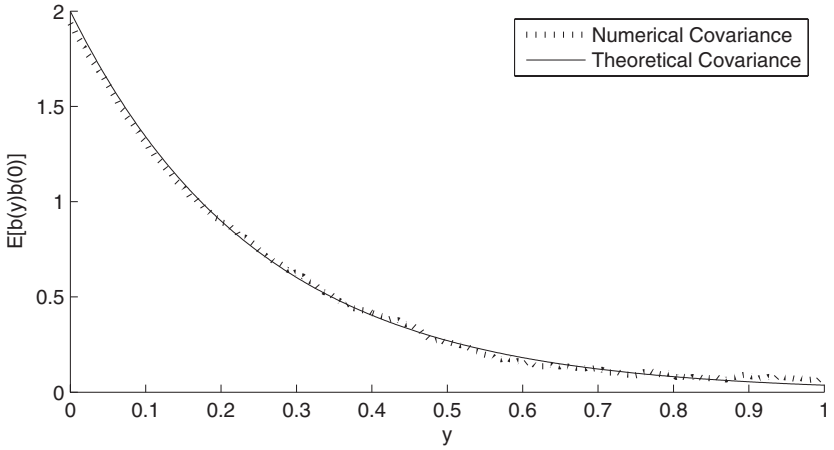

Figure 4. Numerical and exact covariance functions of the O–U process $b(y, \omega)$.

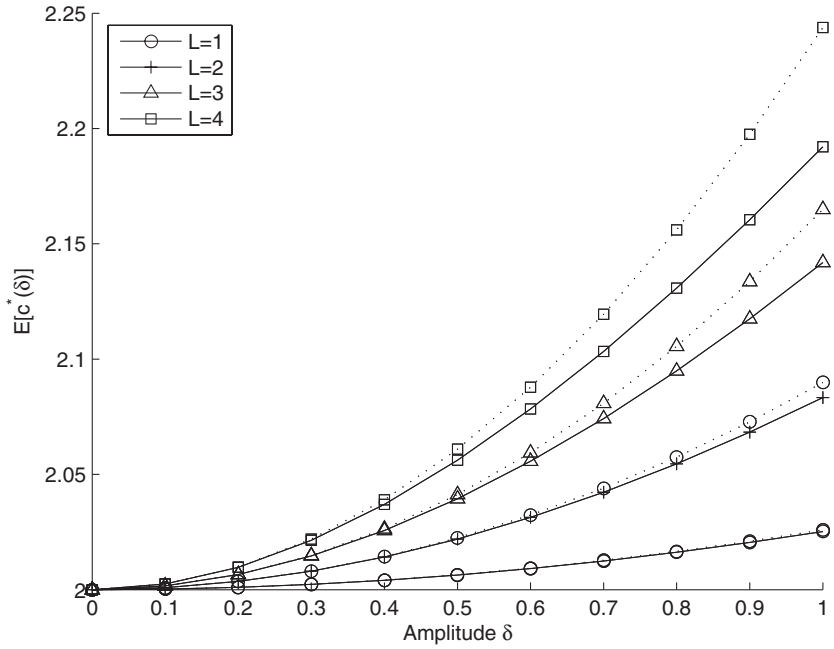

Figure 5. Average enhancement of minimal speed in small amplitude shears. The solid curves are the numerically computed values and the dotted curves are given by formula (2.39).

and $g_1 < g_2$, provided that $\sqrt{\kappa/f'(0)}$ is sufficiently small, depending on the realization. In figure 7 we compare the distributions for $c^*(50)$, g_1 and g_2 for $\kappa = 0.01$. The asymmetry is seen in all three curves.

3.2.2. Dependence on covariance. Next, we consider the effect of the covariance on the enhancement of the minimal speed. The covariance $E[b(y)b(s)]$ is a function of $|t| = |s - y|$,

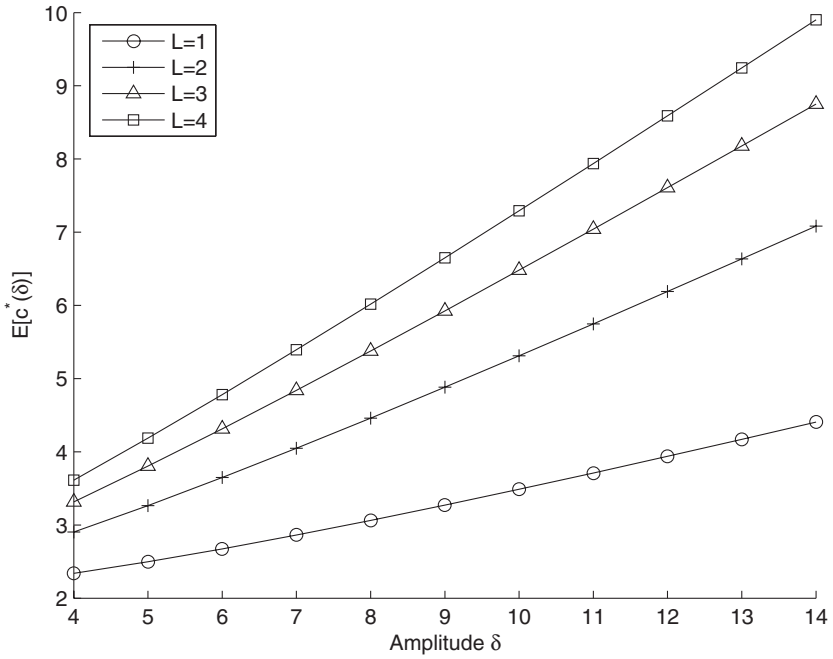

Figure 6. Average enhancement of minimal speed and large amplitude shears.

Table 1. Computed scaling exponents p for $E[c^*(\delta)] = c_0^* + O(\delta^p)$.

	$L = 1.0$	$L = 2.0$	$L = 3.0$	$L = 4.0$
$\delta \ll 1$	2.00	1.98	1.96	1.93
$\delta \gg 1$	1.09	1.05	1.04	1.03

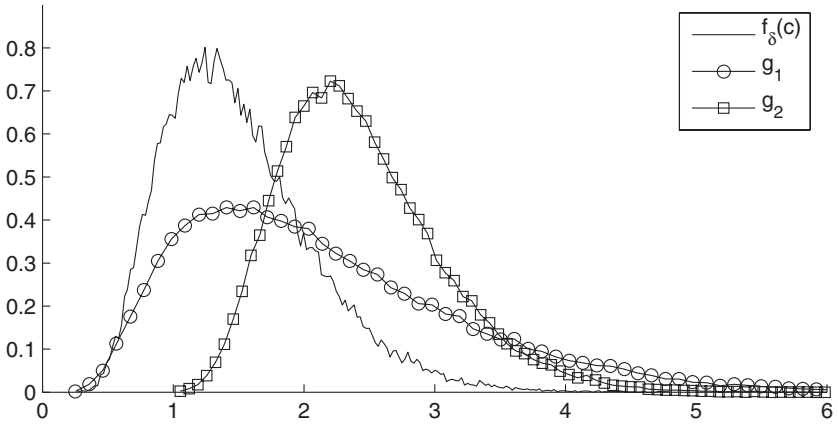

Figure 7. Distributions of speed enhancement and lower and upper bounds at $\delta = 50$.

and so we will write $V(t) = E[b(y)b(s)]$. By choosing $r = \sqrt{2}\alpha^{3/4}$, we constructed O–U processes with covariances given by

$$V(t) = \sqrt{\alpha}\mathrm{e}^{-\alpha|t|}. \tag{3.4}$$

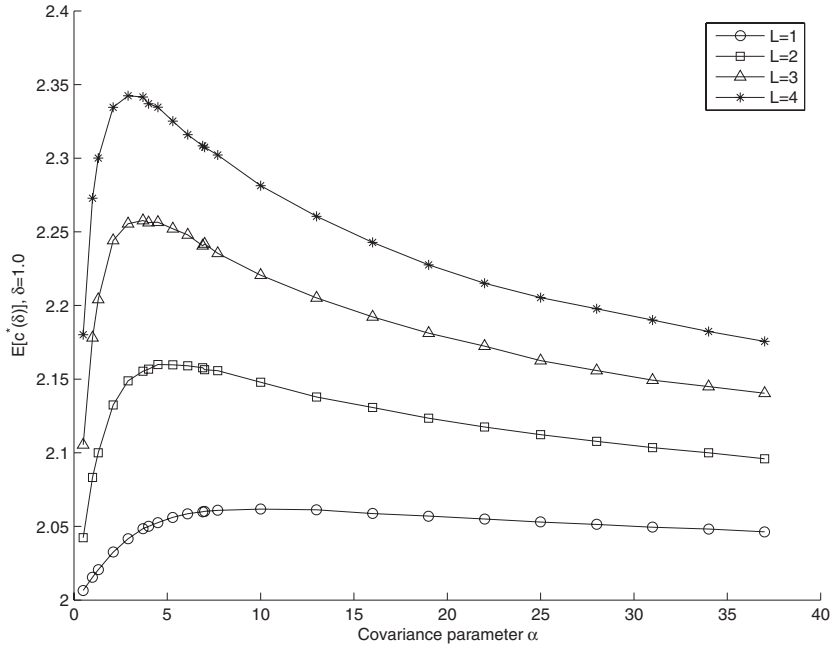

Figure 8. Effect of covariance on minimal speed enhancement at $\delta = 1.0$.

By this choice of r, the L^2 norm of $V(t)$ remains constant as α changes, so that the total energy in the power spectrum of the signal remains constant. Since $r^2/2a = \sqrt{a}$, we see from equation (2.39) that for fixed L,

$$\lim_{\alpha\to+\infty} E[\langle|\chi_x|^2\rangle] = \lim_{\alpha\to 0^+} E[\langle|\chi_x|^2\rangle] = 0 \tag{3.5}$$

and that $E[\langle|\chi_x|^2\rangle]$ attains a maximum for some finite value of $\alpha \in (0,\infty)$. This suggests that there is some optimal α, depending on the domain size L, such that the enhancement of $E[c^*(\delta)]$ is maximized.

Fixing the grid spacing $\mathrm{d}x = 0.002$, we computed the expected value $E[c^*(\delta)]$ for a range of α and for $L = 1.0, 2.0, 3.0, 4.0$. Note that for each α, we must choose the initial points b_0 to have variance $E[b_0^2] = \sqrt{\alpha}$ so that the process remains stationary for each α. Varying the covariance does not affect the order of the scaling in δ. That is, in each case the enhancement scales like $O(\delta^2)$ for small δ and $O(\delta)$ for large δ, as in the preceding simulation.

Figure 8 shows the enhancement $E[c^*(\delta)]$ for a fixed $\delta = 1.0$ and a range of α. Figure 9 shows the results of the same computation for $\delta = 15.0$, corresponding to the large δ regime. In this case, formula (2.39) is no longer valid. Nevertheless, we see the same effect as in the small amplitude regime: the existence of an optimal covariance parameter α.

This effect can be interpreted in terms of $V(t)$ and its Fourier transform or power spectrum:

$$\hat{V}(w) = \sqrt{\frac{2}{\pi\alpha}}\left(1 + \left(\frac{w}{\alpha}\right)^2\right)^{-1}. \tag{3.6}$$

As $\alpha \to 0$, $\hat{V}(w)$ concentrates at the origin, and so the energy of the shear process is concentrated more in the large scale spatial modes. The domain Ω, to which the process is restricted, is bounded, and variations over a length scale that is much greater than the diameter of Ω have little effect on the average enhancement of the front. As a result, $E[c^*]$

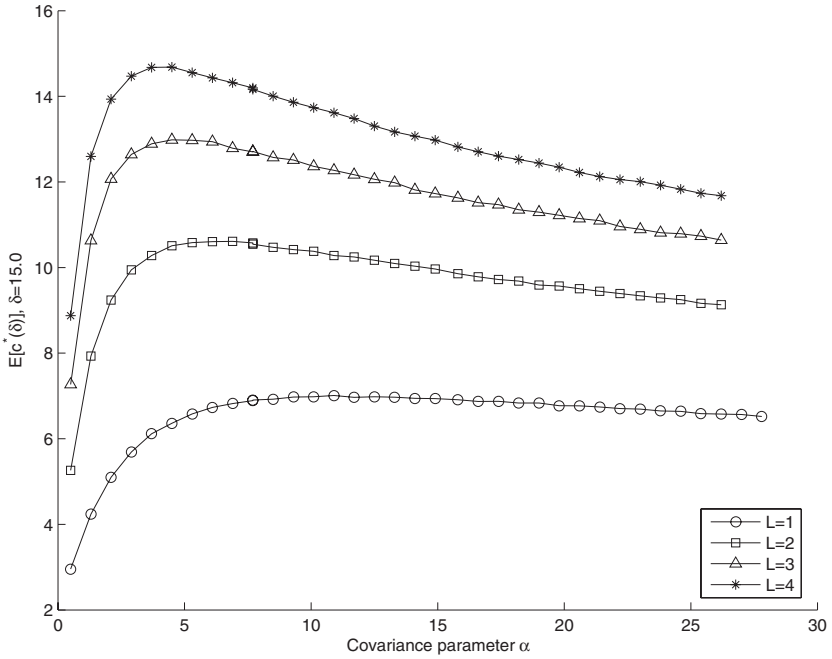

Figure 9. Effect of covariance on minimal speed enhancement at $\delta = 15.0$.

decreases as $\alpha \to 0^+$. In the other limit, $\alpha \to \infty$, $\hat{V}$ spreads out so that the energy over any finite band of frequencies goes to zero, causing $E[c^*]$ to decrease as well. Note that $V \to 0$ in L^1 as $\alpha \to \infty$, and so even though $\hat{V}$ spreads out more uniformly as $\alpha \to 0$, the family of processes does not converge to white noise, whose covariance function is equal to the Dirac delta function.

3.2.3. Speed distribution. For a fixed $\delta = 1$ and $\delta = 14$ (corresponding to small and large amplitudes), we computed the distributions of the numerically computed values $M(\delta)$. The distributions are shown in figure 10. To compute these distributions, we partition the range of values into Q disjoint intervals: $\{[x_j, x_{j+1})\}_{j=1}^{Q}$. Then, we let

$$\mathrm{pdf}(x) = \frac{1}{N} \sum_{i=1}^{N} \frac{\chi_j(M_i(\delta))}{(x_{j+1} - x_j)} \qquad \text{if } x \in [x_j, x_{j+1}), \tag{3.7}$$

where $\chi_j(x)$ is the characteristic function of the interval $[x_j, x_{j+1})$. The distributions in figure 10 were computed with $N = 100\,000$ samples and $Q = 300$.

The values $M(\delta)$ are the enhancement of the minimal speeds due to the variation of the shear, after the effect of the mean field has been subtracted. Since a mean zero shear always enhances the minimal speeds, we should expect $M(\delta) > 0$ for all δ, for all realizations. As already noted, figure 11 shows good convergence of the distributions when using $N = 100\,000$ samples.

3.2.4. Comparison with direct simulation. When comparing the results of the previous sections with results from direct simulation, we find that computing the minimal speeds using the variational formula offers significant advantages. As in [22], we first computed

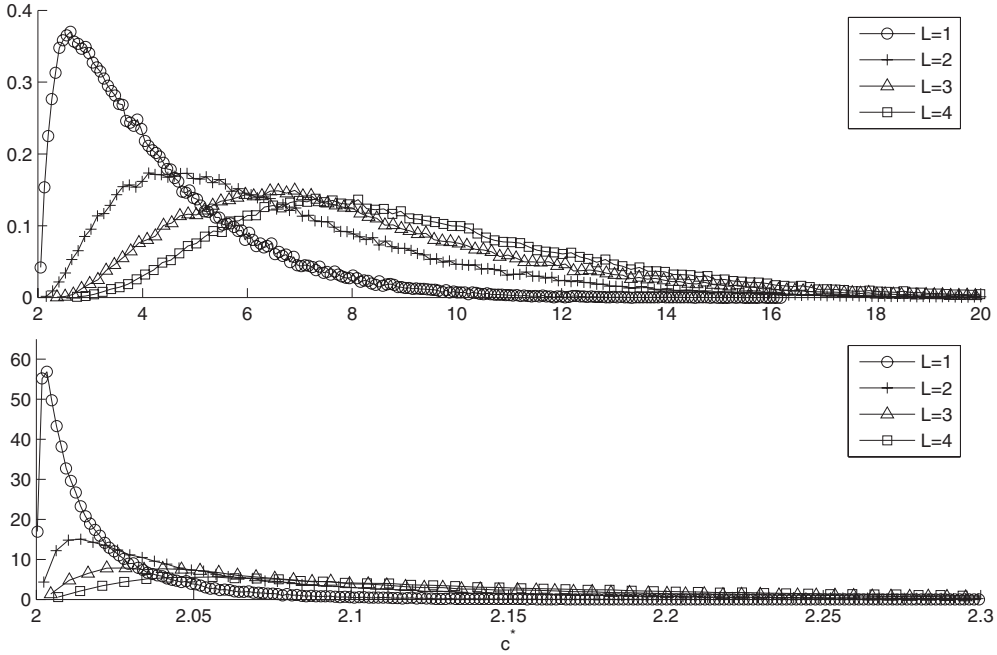

Figure 10. Computed probability distribution functions (pdfs) of enhancement $M(\delta)$: $\delta = 1.0$ (bottom), $\delta = 14.0$ (top).

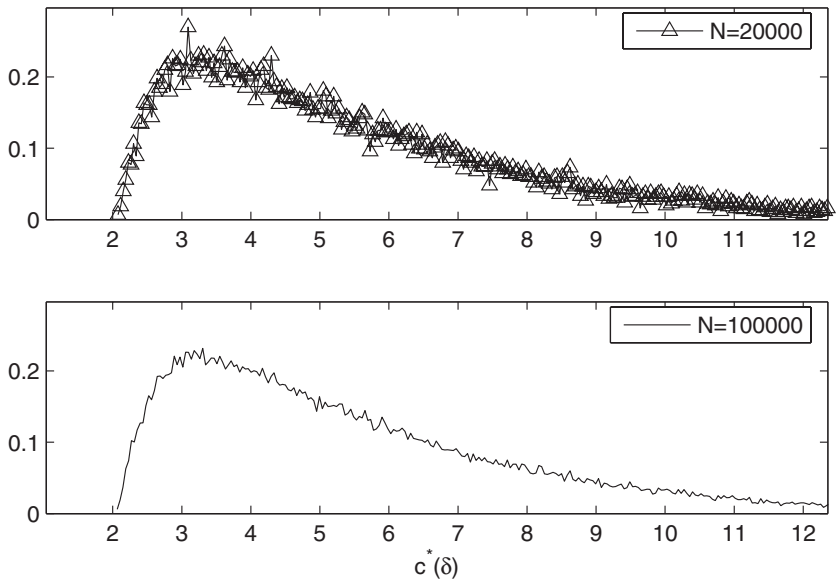

Figure 11. Convergence of speed enhancement distribution at $\delta = 14.0$.

the quantities $E[c^*(\delta)]$ via direct simulation of the original equation (1.1) on a truncated domain using an explicit second order upwind finite-difference scheme. We chose the diffusion constant in the direct simulations to be $\kappa = 0.025$ and the grid spacing to be $\mathrm{d}x = 0.05$, $\mathrm{d}t = 0.004$. For each realization of the shear, we evolved the solution of (1.1) for a sufficiently

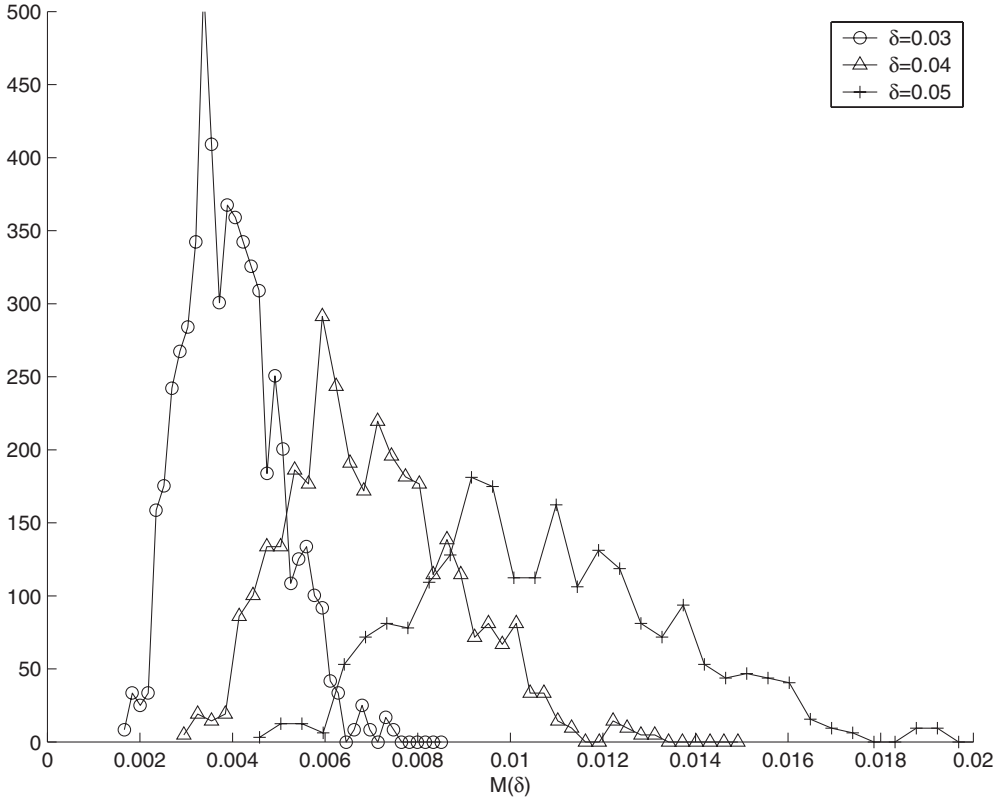

Figure 12. Distribution of speed enhancement via direct simulation, KPP nonlinearity, $\delta = 0.5$.

long time until the front moved at a more or less constant speed (see [22] for details of the method). In this way, we approximated the minimal speed for each realization; then we repeated the process for a large ensemble of shears to compute the expectations $E[c^*(\delta)]$.

We considered three nonlinearities in our direct simulations:

- KPP nonlinearity: $f(u) = u(1-u)$.
- Combustion nonlinearity: $f(u) \equiv 0$ for $u \in [0, \theta]$, and $f(u) > 0$ for $u \in (\theta, 1]$, for some $\theta \in (0, 1)$. Also, $f'(1) < 0$.
- Bistable nonlinearity: $f(u) = u(1-u)(u-\mu)$ for some $\mu \in (0, 1/2)$.

Although there is no known variational formula as simple as formula (1.2) for the bistable and combustion nonlinearities, the expansion (2.5) holds for each of the nonlinearities (see also theorem 4.2 of [13]). Therefore, we should expect that for small δ, the computed values

$$\frac{M(\delta, \omega)}{c_0^*} \approx \frac{\delta^2}{2|\Omega|} \int_\Omega |\nabla \chi(y, \omega)|^2 \, \mathrm{d}y + O(\delta^3) \tag{3.8}$$

have approximately the same distribution, independent of the nonlinearity. For each nonlinearity, we computed more than 700 realizations of the shear and evolved the solution, as described in [22]. The relatively smaller number of samples was due to the long time required to compute each sample (not a problem with the variational formula in the KPP case). After subtracting the linear part of the enhancement (due to the mean field),

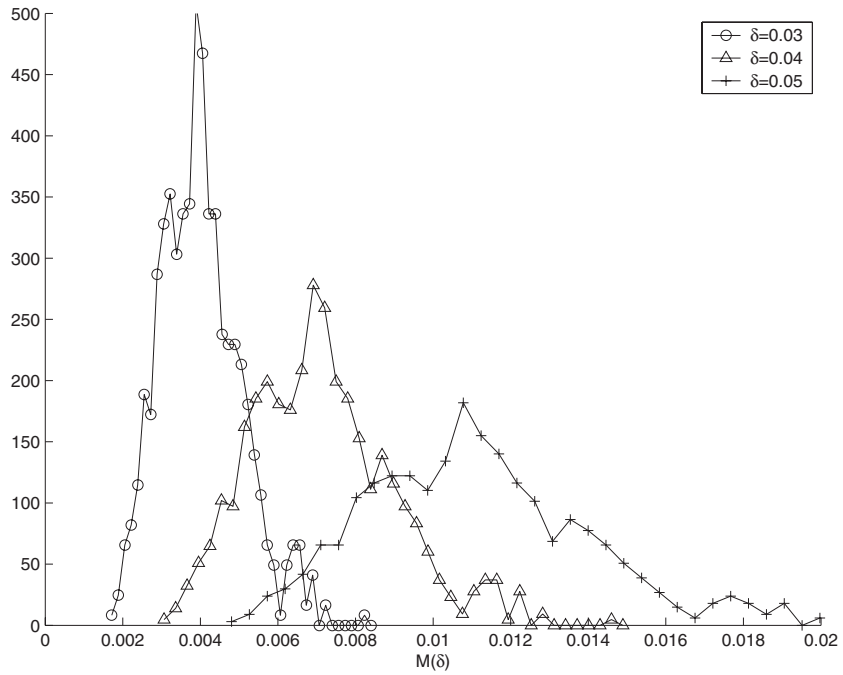

Figure 13. Distribution of speed enhancement via direct simulation, combustion nonlinearity, $\delta = 0.5$.

we computed the enhancement exponent as described in section 3. The results of the direct simulation confirm that, for small amplitudes, $E[c^*(\delta)]$ scales like $O(\delta^2)$. Figures 12–14 show the distributions of the computed values $M(\delta)/c_0^*$ for the KPP, combustion and bistable nonlinearities, respectively, for $L = 1$. We see that the distributions are roughly the same, independent of the nonlinearity, as should be expected. While computationally expensive, the direct simulation method reveals the universal $O(\delta^2)$ scaling of the front speeds for small δ (albeit on smaller ensembles than in the variational computations), for each of the nonlinearities considered.

Because the shears are random and may greatly distort the wave front, one major challenge in accurately approximating the (minimal) speeds is tracking the widely varying front region over a long time. In the region of the front, gradients are relatively large, and so accurately tracking the front requires either a very fine uniform grid spanning a large domain or some kind of adaptive-mesh scheme. In either case, accurate direct simulation is prohibitively expensive compared with the simple variational method. In contrast to the direct simulation method, the variational formula allowed us to compute a much larger number of samples in a fraction of the time and avoid the inaccuracies resulting from truncation of the channel domain.

Finally, we note that if Ω is unbounded, then the quadratic asymptotic behaviour of $c^*(\delta)$ cannot hold in general. For example, in [27], it was shown that if the channel $R \times [0, L]$ is replaced by R^2, then the front velocities obtained through a comparable variational principle diverge due to the almost sure growth of the running maximum of the process $b(y, \omega)$. This effect can be clearly seen in our results, as $E[\langle|\nabla\chi|^2\rangle]$ given by (2.39) diverges as $L \to +\infty$. In our application of theorem 2.1 to a stationary Gaussian process, the boundedness of the domain Ω is crucial for achieving the necessary bound on $\|b\|_\infty$ (through the martingale moment inequality), and in turn the bound on c^*.

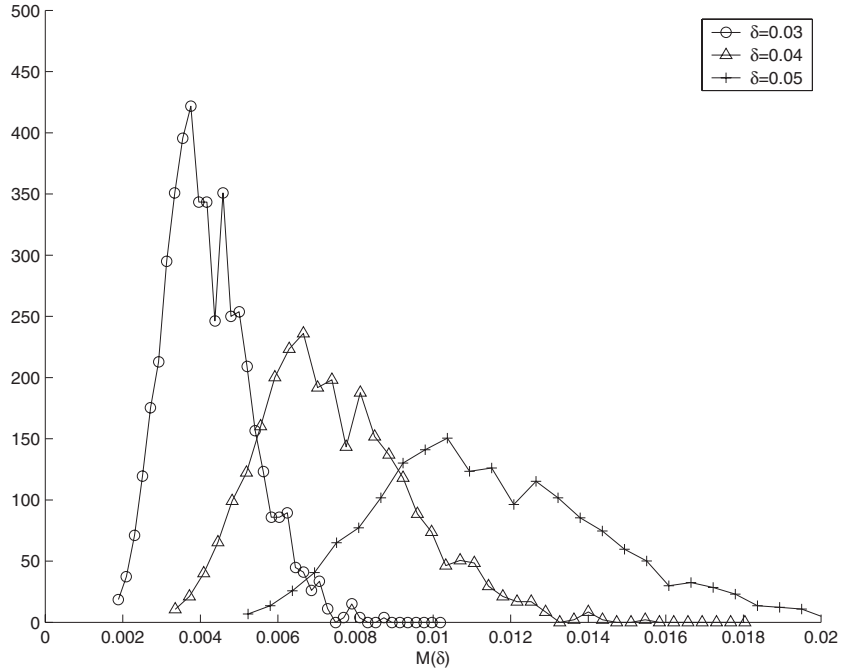

Figure 14. Distribution of speed enhancement via direct simulation, bistable nonlinearity, $\delta = 0.5$.

4. Conclusions

Sufficient moment conditions are obtained to ensure the quadratic (linear) KPP average front speed enhancement through small (large) rms random shear flows in channel domains. The conditions are realized by the O–U process, for which an explicit average front speed formula is derived. The variational principle based computation is carried out for the speed ensemble. The numerically computed speed enhancement is in agreement with theoretical analysis, and provides data for studying speed distributions and the dependence on the shear covariance. Comparison with direct simulations of random fronts in the case of non-KPP nonlinearities showed the same enhancement scaling laws. It would be interesting to investigate front speeds through time dependent random shear flows or nonshear random flows in channel domains for future studies.

Acknowledgments

The work was partially supported by NSF grant ITR-0219004. JX would like to acknowledge a fellowship from the John Simon Guggenheim Memorial Foundation, and a Faculty Research Assignment Award at UT Austin. JN is grateful for support through a VIGRE graduate fellowship at UT Austin. Both authors wish to thank J Wehr for helpful communications.

References

[1] Adler R 1980 *The Geometry of Random Fields* (New York: Wiley)
[2] Anderson E *et al* 1999 *LAPACK Users' Guide* 3rd edn (Philedelphia, PA: Society for Industrial and Applied Mathematics)

[3] Audoly B, Berestycki H and Pomeau Y 2000 Reaction–diffusion en ećoulement rapide *C. R. Acad. Sci., Paris* II **328** 255–62
[4] Berestycki H 2003 The influence of advection on the propagation of fronts in reaction–diffusion equations *Nonlinear PDEs in condensed Matter and Reactive Flows* (*NATO Science Series C* vol 569) ed H Berestycki and Y Pomeau (Dordrecht: Kluwer)
[5] Berestycki H and Hamel F 2002 Front propagation in periodic excitable media *Commun. Pure Appl. Math.* **60** 949–1032
[6] Berestycki H and Nirenberg L 1992 Travelling fronts in cylinders *Ann. Inst. H Poincare, Anal. Nonlineaire* **9** 497–572
[7] Clavin P and Williams F A 1979 Theory of premixed-flame propagation in large-scale turbulence *J. Fluid Mech.* **90** 598–604
[8] Constantin P, Kiselev A, Oberman A and Ryzhik L 2000 Bulk burning rate in passive–reactive diffusion *Arch. Rat. Mech. Anal.* **154** 53–91
[9] Friedman A 1969 *Partial Differential Equations* (New York: Holt, Reinhart and Winston)
[10] Gilbarg D and Trudinger N 1983 *Elliptic Partial Differential Equations of Second Order* 2nd edn (Berlin: Springer)
[11] Heinze S 2001 The speed of traveling waves for convective reaction diffusion equations *Preprint* 84 MPI, Leipzig
[12] Heinze S 2005 Large convection limits for KPP fronts *Preprint* 21 MPI, Leipzig
[13] Heinze S, Papanicolaou G and Stevens A 2001 Variational principles for propagation speeds in inhomogeneous media *SIAM J. Appl. Math.* **62** 129–48
[14] Karatzas I and Shreve S 1991 *Brownian Motion and Stochastic Calculus (Graduate Texts in Mathematics)* 2nd edn (Berlin: Springer)
[15] Kerstein A R and Ashurst W T 1992 Propagation rate of growing interfaces in stirred fluids *Phys. Rev. Lett.* **68** 934
[16] Kiselev A and Ryzhik L 2001 Enhancement of the traveling front speeds in reaction–diffusion equations with advection *Ann. Inst. H Poincaré, Anal. Nonlinéaire* **18** 309–58
[17] Kloeden P and Platen E 1999 *Numerical Solution of Stochastic Differential Equations* (Berlin: Springer)
[18] Khouider B, Bourlioux A and Majda A 2001 Parameterizing turbulent flame speed—Part I: unsteady shears, flame residence time and bending *Combust. Theory Modelling* **5** 295–318
[19] Majda A and Souganidis P 1994 Large scale front dynamics for turbulent reaction–diffusion equations with separated velocity scales *Nonlinearity* **7** 1–30
[20] Majda A and Souganidis P 1998 Flame fronts in a turbulent combustion model with fractal velocity fields *Commun. Pure Appl. Math.* L**I** 1337–48
[21] Nolen J and Xin J 2004 Existence of KPP type fronts in space-time periodic shear flows and a study of minimal speeds based on variational principle *Preprint* math. AP/0407366 (2005 *Discrete Cont. Dyn. Syst.* at press)
[22] Nolen J and Xin J 2003 Reaction diffusion front speeds in spatially–temporally periodic shear flows *SIAM J. Multiscale Modelling Simul.* **1** 554–70
[23] Papanicolaou G and Xin J 1991 Reaction–diffusion fronts in periodically layered media *J. Stat. Phys.* **63** 915–31
[24] Ronney P 1995 Some open issues in premixed turbulent combustion *Modelling in Combustion Science* (*Lecture Notes in Physics* vol 449) ed J D Buckmaster and T Takeno (Berlin: Springer) pp 3–22
[25] Vladimirova N, Constantin P, Kiselev A, Ruchayskiy O and Ryzhik L 2003 Flame enhancement and quenching in fluid flows *Combust. Theory Modelling* **7** 487–508
[26] Xin J 2000 Front propagation in heterogeneous media *SIAM Rev.* **42** 161–230
[27] Xin J 2003 KPP front speeds in random shears and the parabolic Anderson problem *Methods Appl. Anal.* **10** 191–8
[28] Yakhot V 1988 Propagation velocity of premixed turbulent flames *Combust. Sci. Technol.* **60** 191